

1 **Direct Glycan Analysis of Biological Samples and Intact Glycoproteins by**
2 **Integrating Machine Learning Driven- Surface-Enhanced Raman Scattering**
3 **(SERS) and Boronic Acid Array**

4 Qiang Hu¹, Hung-Jen Wu^{1,*}

5 ¹ The Artie McFerrin Department of Chemical Engineering, Texas A&M University, TX
6 77843, USA

7 * Corresponding author

8 ***Abstract***

9 Frequent monitoring of glycan patterns is a critical step for studying glycan-mediated
10 cellular processes. However, the current glycan analysis tools are resource-intensive and
11 less suitable for routine use in standard laboratories. We developed a novel glycan detection
12 platform by integrating surface-enhanced Raman spectroscopy (SERS), boronic acid (BA)
13 receptors, and machine learning (ML) tools. This sensor monitors the molecular fingerprint
14 spectra of BA binding to cis-diol-containing glycans. Different types of BA could yield
15 different stereoselective reactions toward different glycans and exhibit unique vibrational
16 spectra. By integrating the Raman spectra collected from different BA receptors, the
17 structural information can be enriched, eventually improving the accuracy of glycan
18 classification and quantification. Here, we established a SERS-based sensor incorporating
19 multiple different BA receptors. This sensing platform could directly analyze the biological
20 samples, including the whole milk and intact glycoproteins (fetuin and asialofetuin),
21 without tedious glycan release and purification steps. The results demonstrate the
22 platform's ability to classify milk oligosaccharides with remarkable classification accuracy,
23 despite the presence of other non-glycan constituents in the background. This sensor could
24 also directly quantify sialylation levels of fetuin/asialofetuin mixture without glycan
25 release procedures. Moreover, by selecting appropriate BA receptors, the sensor exhibits
26 an excellent performance of differentiating between α 2,3 and α 2,6 linkages of sialic acids.
27 This low-cost, rapid, and highly accessible sensor will provide the scientific community
28 with an invaluable tool for routine glycan screening in standard laboratories.

1 **Introduction:**

2 Glycans are highly abundant biomolecules found in all living organisms. They form dense
3 layers on cell membranes, proteins, and other biomolecules, facilitating a wide range of
4 biochemical reactions¹. The glycosylation processes are highly sensitive to various factors,
5 such as environmental conditions, cell activities, nutrition, cell growth cycles, cell health,
6 etc^{2, 3}. To investigate glycan-mediated cellular processes, frequent monitoring of glycan
7 changes in biological samples is essential. However, glycan analysis poses significant
8 challenges due to their intricate structures, including complex isomeric forms, glycosidic
9 linkages, and branched structures.

10 The comprehensive glycan sequencing tools, such as mass spectrometry (MS)-based
11 techniques, are effective but highly resource-intensive; therefore, these methods are less
12 suitable for routine use in standard laboratories^{4,6}. Staining samples with lectins (i.e.,
13 glycan binding proteins) is another popular tool for comparative glycan analysis. Because
14 the protocol is relatively simple, lectin staining can be applied in standard laboratories⁷.
15 However, lectin-glycan interactions are not highly specific⁸⁻¹¹; a lectin often binds to
16 various glycan structures with different affinities¹²⁻¹⁴. In addition, the relatively small lectin
17 library could not cover all of the essential glycan structures. Thus, there is a growing
18 demand for a low-cost, rapid, and highly accessible tool that empowers researchers to
19 frequently monitor dynamic changes in glycosylation^{4,6}.

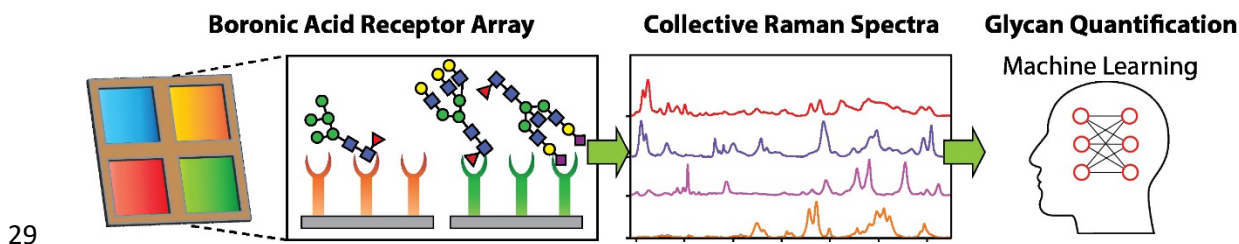
20 Our prior research developed a machine learning (ML)-driven surface enhanced Raman
21 spectroscopy (SERS) sensor capable of classifying the selected glycans with remarkable
22 accuracy exceeding 99%¹⁵. This new sensing platform includes three major components:
23 (1) boronic acid (BA) receptors, (2) SERS, and (3) ML program. (Scheme shown in Figure
24 1) BA can reversibly bind with cis-diol-containing carbohydrates, leading to the formation
25 of boronate esters¹⁶. It is worth noting that BA binding is not highly specific to a particular
26 glycan structure. Thus, the classic yes/no confirmative response (e.g., fluorescence) in the
27 staining assay is not sufficient to distinguish different glycan structures. To further identify
28 the glycan structures, the sensor monitors molecular fingerprint spectra of BA-glycan
29 reaction complex.

30 Raman spectroscopy was chosen to monitor molecular fingerprint spectra for several
31 reasons. First, Raman spectroscopy not only provide fingerprint information of molecules
32 but also can distinguish isomeric structures, allowing for isomeric glycan detection¹⁷.
33 Second, the availability of low-cost Raman spectrometers will enable widespread
34 adoption¹⁸. Additionally, a low-cost plasmonic SERS substrate (<\$0.08 per test), called
35 nanopaper, are used to enhance Raman signals^{19, 20}.

36 In our previous work, we had evaluated two commercially available BA receptors, namely
37 4-mercaptophenylboronic acid (4MBA) and 1-thianthrenylboronic acid (1TBA), which
38 effectively captured glycan molecules through cis-diol chemical reactions¹⁵. Utilizing
39 advanced ML algorithms, we analyzed spectral variations across a wide frequency range
40 for glycan detection. This sensor successfully distinguished stereoisomers and structural
41 isomers featuring different glycosidic linkages.

1 One of the key observations in our previous study is that the structural information of
2 glycans can be enriched by integrating the spectra obtained from 4MBA and 1TBA. The
3 collective Raman spectra could increase the accuracy of glycan classification and
4 quantification. This discovery offers a strategy to improve the sensor performance by using
5 an array of BA receptors. Here, we developed a glycan sensor containing up to 8 different
6 BA receptors to directly analyze the complex biological samples without glycan
7 purification steps, including whole milk and intact glycoproteins. Because SERS is a near-
8 field phenomenon, the resulting Raman signals primarily originate from BA-glycan
9 reaction complexes that are directly adsorbed on metallic nanoparticles. The influences of
10 the background matrices were minimal. As expected, the collective spectra from different
11 BA receptors achieved a remarkable 100% accuracy for classifying the milk
12 oligosaccharides in the commercial dairy products.

13 In addition, we used this platform to directly analyze intact glycoproteins. Protein
14 glycosylation analysis typically requires tedious sample preparation, such as enzymatically
15 releasing glycans from glycoproteins and chemically labeling glycans for detection²¹⁻²³.
16 Direct analysis of intact glycoproteins will speed up the analysis procedure and benefit the
17 glycobiology community. We evaluated the feasibility of quantifying sialylation levels of
18 fetuin/asialofetuin mixture. The collective spectra once again demonstrated superior
19 quantification performance, with R^2 and normalized mean square error (NMSE) values of
20 0.9941 and 0.005912, respectively. Moreover, we evaluated the sensor performance in
21 distinguishing glycosylic linkages of sialic acids. Sialic acid is an important
22 monosaccharide for mammals due to its functionality in nervous system development,
23 immune regulation, and involvements in many diseases²⁴⁻²⁶. We tested the sensor's
24 classification performance on the most common $\alpha 2,3$ and $\alpha 2,6$ sialic acid linkage^{27, 28}. By
25 using various BA receptors, the sensor could achieve 100% accuracy in the classification
26 of sialic acid linkages. In summary, this sensor could work as a user-friendly platform to
27 directly detect glycan profiles in biological samples and intact glycoproteins without time-
28 consuming glycan purification steps.



30 *Figure 1. Schematic of the sensor. Glycans are captured by various boronic acids (BAs) printed on the SERS substrates.*
31 *Each BA-glycan reaction complex offers a unique molecular fingerprint spectrum. The structural information is enriched*
32 *by integrating the fingerprint spectra from different BAs, called the collective Raman spectra. The complex collective*
33 *spectra are processed by the advanced machine learning technique for glycan classification and quantification.*

34

1 **Methods:**

2 **Materials:**

3 2-(N-morpholino)ethanesulfonic acid (MES), fetuin, asialofetuin, 2,3 sialyllactose (3-
4 SLA), *N*-acetylneuraminic acid (Neu5Ac/sialic acid), 2,6 sialyllactose (6-SLA), 4-
5 mercaptophenylboronic acid (4MBA), 1-thianthrenylboronic acid (1TBA), 3-
6 mercaptophenylboronic acid (3MBA), 4-aminophenylboronic acid (4ABA), pyridine-4-
7 boronic acid (PyriBA), pyrene-1-boronic acid (PyreBA), 2-(hydroxymethyl)phenylboronic
8 acid cyclic monoester (HBACM), and benzo[*b*]thien-2-ylboronic acid (BBA) were
9 purchased from Sigma Aldrich (boronic acid structure are shown in SI Figure 1). Glass
10 microfiber paper (GF-C, binder free, 100 mm circles) was acquired from Whatman. Silver
11 nitrate (99.99995%), ammonia, dextrose and 2-propanol were purchased from
12 ThermoFisher scientific. All milk products were purchased from local markets. All
13 chemicals were ACS grade or higher and used without further purification.

14

15 **Nanopaper fabrication:**

16 Nanopapers were fabricated as previously reported^{15, 19, 20}. In brief, Tollens' reagent
17 containing 300 mM ammonia and 50 mM silver nitrate was prepared in a 2 L glass beaker
18 in a 55 °C water bath. Glass microfiber papers were immersed in the solution, and 500 mM
19 glucose solution was added to initiate the silver mirror reaction. After the reaction was
20 complete, the filter papers were rinsed thoroughly with deionized water and 2-propanol.
21 The resulting products, i.e., the nanopapers, were stored in 2-propanol at room temperature.
22 The storage container was covered with aluminum foil and placed in drawers to prevent
23 light exposure.

24

25 **Surface modification**

26 The surface modification was performed as previously reported¹⁵. In brief, nanopapers
27 were cut into a 1 cm × 0.5 cm rectangular shape, and then immersed in 50 mM 1TBA or
28 0.1 mM for other boronic acids (BAs) in methanol for 1 hour. Before glycan measurement,
29 the BA-coated nanopaper was air-dried. For the glycan measurement, the BA-coated
30 nanopapers were spotted with the aqueous solutions containing glycans or glycoproteins in
31 100 mM MES buffer (pH 5) and incubated for 1 hour. Before Raman measurement, the
32 paper was dried in an oven at 75°C for 5 minutes.

33

34 **Raman measurement**

35 Raman spectra were collected with a ThermoFisher Scientific DXR3 Raman microscope
36 using laser excitation with a wavelength of 785 nm and an output power of 1 mW. This
37 instrument was equipped with an Olympus BX41 optical microscope and a

1 thermoelectrically cooled charge-coupled detector (ThermoFisher front-illuminated CCD
2 system) with 1024 × 256 pixel format, operating at −70 °C. The signal was calibrated by
3 an internal polystyrene standard and a 10× objective. The spot size was about 3.8 μm. 200
4 SERS spectra were collected with an exposure time of 1 s for 5 accumulations at different
5 spots for each sample.

6

7 **Milk oligosaccharide extraction and classification**

8 The milk oligosaccharide was extracted using the traditional Folch extraction with slight
9 modification²⁹. Briefly, the milk was mixed with chloroform and methanol mixture (3:1,
10 v/v) in a 1:4 (milk v/solvent v) ratio in the 50mL Nalgene™ Oak Ridge high-speed PTFE
11 FEP centrifuge tubes. The mixture was shaken vigorously for 5 minutes until homogeneous,
12 followed by 40 minutes of centrifuge at 4000 RPM. The upper layer of the solution was
13 extracted and concentrated in the rotary evaporator under 55 °C until all solvents were
14 evaporated. Total carbohydrate concentration was determined using the phenol-sulfuric
15 acid assay³⁰. The absorbance of the carbohydrate assay was detected by microplate reader
16 (BMG Labtech FLUOstar Omega). After that, the oligosaccharide extracts were stored at
17 −20 °C until usage. Three extractions were performed on each milk type on different days.

18 The dried milk oligosaccharide extracts were reconstituted with DDI water to reach the
19 final total carbohydrate concentration of 0.34 mg/mL, which is the same concentration as
20 the 1 mM lactose solution. The reconstituted oligosaccharide samples were measured under
21 the same protocol as above, with 600 spectra collected for each milk type. Before data
22 analysis, the spectra were averaged for three batches, resulting in 200 spectra for each milk
23 type.

24

25 **Whole milk glycan profiling**

26 20 μL of cow milk, goat milk, oat milk, soy milk, or almond milk was spotted onto surface-
27 modified nanopaper using micropipettes and left for 1 hour. The paper was then rinsed with
28 100 mM MES buffer (pH 5) to remove unbound proteins and non-glycan contents.
29 Subsequently, the paper dried in an oven at 75°C for 5 minutes and was measured by Raman
30 spectrometer using the protocol reported above.

31

32 **Intact protein quantification**

33 Different ratios of 1 mM fetuin and 1 mM asialofetuin in 100 mM MES buffer (pH 5) were
34 mixed at different ratios to prepare a titration curve ranging from 0% to 100% of 1 mM
35 fetuin, with 20% intervals. The glycoprotein mixtures were spotted on the BA-coated
36 nanopapers and incubated at room temperature for 1 hour. The nanopaper was then dried

1 in an oven at 75°C for 5 minutes and measured by Raman spectrometer using the same
2 protocol as above.

3

4 **Sialic acid linkage identification**

5 Aqueous solutions of 1 mM of 2,3 sialyllactose (3-SLA), 1 mM of 2,6 sialyllactose (6-
6 SLA), and an equal volume mixture of sialic acid (0.5 mM) and lactose (0.5 mM) were
7 prepared to represent α 2,3 sialic linkage, α 2,6 sialic acid linkage, and no linkage between
8 sialic acid and other glycans, respectively. The samples were spotted on the BA-coated
9 nanopapers and incubated at room temperature for 1 hour. Afterward, the nanopaper was
10 then dried in an oven at 75°C for 5 minutes and measured by Raman spectrometer using
11 the same protocol reported above, with 200 spectra collected for each concentration.

12

13 **Data processing**

14 The data analysis was performed using the same methodology reported in the previous
15 study¹⁵. Briefly, the spectra were first processed using asymmetric least square (ALS)
16 baseline correction. Then, baselined spectra were vector normalized and smoothed using
17 Savitzky–Golay filtering (4th order polynomial, with a frame size of 37). Finally,
18 multivariate analysis techniques and classification algorithms were applied in the spectral
19 range 400–1650 cm⁻¹. Data processing was carried out using Matlab 2021b.

20

21 **Multivariate analysis and machine learning**

22 Prior to applying classifiers, the smoothed spectra underwent multivariate statistical
23 analysis to reduce complexity and extract significant spectral features explaining the most
24 variance. Discriminant analysis of principal components (DAPC) was used for this
25 purpose³¹. Principal component analysis (PCA) was initially applied to reduce the data
26 complexity, and then, a supervised analysis process, discriminant analysis, was used to
27 further discriminate the dataset by correlating data variation with the sample information.

28 After feature extraction, common machine learning classifiers were used to classify SERS
29 spectra. Support vector machine (SVM) was selected due to its superior performance in the
30 prior Raman study³². A 5-fold cross-validation was conducted to assess the suitability of
31 the classification algorithm³³. In brief, the training and the validation sets were established
32 by randomly selecting from the Raman spectral data. The training dataset was used to
33 generate a classification model, and the model predicted the validation dataset to evaluate
34 the performance. The cross-validation approach was repeated five times, wherein the
35 validation set consists of and 800 and 480 randomly selected SERS spectra in repetition
36 for the whole milk glycan study and sialic acid linkage study, respectively. The model's
37 performance was evaluated by using classification accuracies, sensitivity, and selectivity.
38 The collective spectra were constructed by combining the truncated boronic acid spectra

1 (400-1650 cm⁻¹). Then, the collective spectra went through the same multivariate analysis
2 and classification algorithm as the individual spectra.

3 Regression analysis was conducted using Matlab 2021b. The gaussian process regression
4 model was used to predict the percentage fraction of fetuin within the fetuin/asialofetuin
5 mixture. DAPC was first performed on the dataset for the wavenumber from 400-1650 cm⁻¹
6 ¹, and then the resulting canonicals were used in regression analysis. A 5-fold cross-
7 validation was performed on the model to evaluate the regression performance. The model
8 was evaluated based on the normalized mean square error (NMSE) and coefficient of
9 determination (R²). For the collective spectra regression, the dataset was built in the same
10 way as described in the classification. Then the spectra went through the same regression
11 algorithm and were evaluated based on the same performance metrics (NMSE and R²).

12 13 **Statistical analysis**

14 The data analysis was performed using the same methodology reported in the previous
15 study¹⁵. For classification tasks, the performance was evaluated by accuracy, sensitivity,
16 and selectivity. The classification accuracy, sensitivity, and selectivity are defined as:

$$17$$
$$18 \text{ Accuracy} = \frac{\text{True positive} + \text{True negative}}{\text{All cases}}(1)$$

$$19 \text{ Sensitivity} = \frac{\text{True positive}}{\text{True positive} + \text{False negative cases}}(2)$$

$$20 \text{ Selectivity} = \frac{\text{True negative}}{\text{True negative} + \text{False positive}}(3)$$

21 For quantitative analysis, the performance was evaluated based on the normalized mean
22 square error (NMSE) and coefficient of determination (R²).

$$23$$
$$24 \text{ NMSE} = \frac{\sum_{i=1}^n (\hat{y}_i - y_i)^2}{\sum_{i=1}^n (\hat{y}_i - \bar{\hat{y}})^2}(4)$$

$$25 \text{ R}^2 = 1 - \frac{\sum_{i=1}^n (y_i - \hat{y}_i)^2}{\sum_{i=1}^n (y_i - \bar{y})^2}(5)$$

26 where \hat{y}_i is the predicted values, y_i is the actual values in the dataset, $\bar{\hat{y}}$ is the mean of the
27 predicted values, \bar{y} is the mean of the actual values, and the n is the number of spectra in
28 the dataset.

29

1 **Result and Discussion**

2 **Direct analysis of unprocessed milk samples**

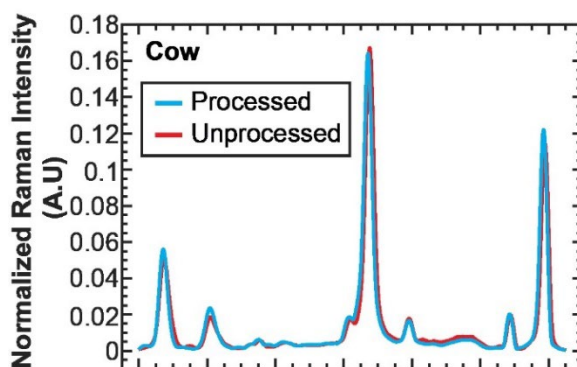
3 Our previous study demonstrated ML-driven SERS platform exhibits exceptional
4 performance on identifying purified glycans¹⁵. However, the additional purification
5 process is time-consuming and may result in the loss and degradation of glycans. A new
6 approach allowing direct analysis of unprocessed biological samples and intact
7 glycoproteins will benefit the scientific communities. For the proof-of-concept, we first
8 evaluate the feasibility of analyzing milk oligosaccharides in the unprocessed milk samples.

9 Milk oligosaccharides are pivotal nutrients in the human health³⁴. For example, sialic acids
10 in milk are critical for supporting infant body development^{35, 36}. Researchers commonly
11 use liquid chromatography-mass spectrometry (LC-MS) to profile N-glycans in milk^{34, 37}.
12 However, the tedious sample preparation and time-consuming testing process limit its
13 widespread use. In our previous study, we have demonstrated the integration of BAs, SERS,
14 and ML program could identify and quantify oligosaccharides extracted from milks. Our
15 approach offers a valuable platform for detecting milk adulteration. However, the
16 oligosaccharide extraction process is time- and labor-intensive. We are now taking a step
17 further to investigate the feasibility of detecting unprocessed milk samples. Direct
18 detection not only reduces the processing time but also eliminates experimental variations
19 during the oligosaccharide extraction process.

20 Because SERS is a near-field effect, we hypothesize that the major Raman signals are
21 contributed by BA-glycan reaction complexes that directly attach to SERS substrates. To
22 verify the hypothesis, we compared the SERS spectra of extracted oligosaccharides and
23 unprocessed milk samples on 4MBA functionalized substrates (Cow milk example shown
24 in Figure 2 & a detailed comparisons among other milk samples in SI Figure 2). Milk was
25 dropped onto a surface-modified nanopaper, and then the nanopaper was rinsed with the
26 buffer to remove unbound proteins and non-glycan contents. The spectral difference
27 between processed and unprocessed milk samples is minimal. The small spectral
28 differences were observed at 470 cm⁻¹ (CCC out of plane bending), 607 cm⁻¹ (CCC in-
29 plane bending), 1075 cm⁻¹ (CCC in-plane bending, CS stretching), and 1589 cm⁻¹ (CC
30 stretching, CH bending). Since the milk oligosaccharides were extracted using Folch
31 method, lipids and proteins were removed during the separation process³⁸. These minor
32 spectral variations are likely contributed by the additional glycan compounds, such as
33 glycoproteins and glycolipids in the unprocessed milk samples. The similarity of SERS
34 spectra between extracted oligosaccharides and unprocessed samples suggests that BA is
35 capable of capturing milk oligosaccharides and the major SERS signals were contributed
36 by BA-glycan reaction complexes, despite the presence of other non-glycan constituents
37 in the background. This discovery allows us to eliminate the time-consuming glycan
38 extraction procedure in the detection protocol.

39 After demonstrating the influence of background molecules is minimal, we evaluated the
40 sensor's capability of classifying commercial dairy products, including cow, goat, soy, oat,
41 and almond milk. In our previous research, we demonstrated that the collective SERS

1 spectra from different BA receptors could enrich the structural information and improve
2 the classification accuracy¹⁵. To improve the sensor performance, we establish an array of
3 BA receptors. This array consists of 5 different BAs, including two BAs used in our
4 previous study (4MBA, 1TBA) and three additional BAs (3MBA, 4ABA, and PyriBA).
5 The position difference of the mercapto group (3MBA vs. 4MBA), the substitution of
6 mercapto group with amine (4MBA vs. 4ABA), and the incorporation of pyridine group in
7 PyriBA could result in distinct molecular vibrations, leading to unique Raman spectra of
8 BA-glycan reaction complexes. The Raman spectra and confusion matrices of these BAs
9 were shown in SI Figure 3 ~ SI Figure 12. Among these BAs, 4MBA exhibited the best
10 performance but still misclassified one sample from all cases. The collective spectra of 5
11 boronic illustrate the remarkable 100% classification accuracy. (SI Figure 13)



12

13 *Figure 2. Average normalized SERS spectra (n=200) of the unprocessed cow milk sample and the purified milk*
14 *oligosaccharides on 4MBA coated substrates. The milk oligosaccharides were extracted from cow milk using Folch*
15 *method. The spectral difference between processed and unprocessed samples is minimal.*

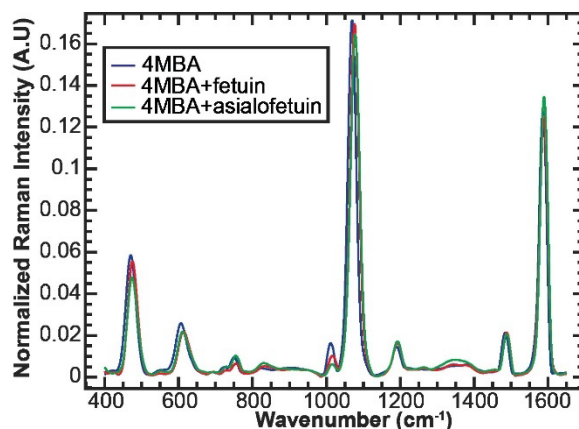
16 **Direct analysis of intact glycoproteins**

17 The current techniques for glycoprotein analysis require tedious sample preparation,
18 including enzymatically releasing glycans from glycoproteins and chemically labeling
19 glycans for detection²¹⁻²³. For example, the glycosidase (PNGase F/PNGase A) could be
20 used to cleave the N-glycans from glycoproteins, and then the glycans are purified via
21 hydrophilic interaction liquid chromatography (HILIC)^{39, 40}. According to the detection
22 techniques, chemical labeling of the glycans may be required for liquid chromatography
23 (LC) or liquid chromatography-mass spectrometry (LC-MS)^{40, 41}. For O-glycan analysis,
24 the procedure can be more complicated due to the lack of enzymatic cleavage methods.
25 While chemical release approaches exist, there is a risk of glycan structure degradation
26 during the release process⁴². Therefore, direct analysis of intact glycoproteins without
27 tedious sample preparation is highly desired. For the proof-of-concept, we selected fetuin
28 and asialofetuin as a model system⁴³. Bovine fetuin is known to contain three N-
29 glycosylation sites and five O-glycosylation sites⁴⁴, while asialofetuin shares the same
30 protein structure and glycosylation sites but lacks terminal sialic acids⁴⁵. Sialic acid plays
31 a crucial role in the central nervous system and the immune system, making it an essential
32 glycan building block²⁴. Here, we used our sensing platform to directly quantify sialylation
33 levels of fetuin/asialofetuin mixtures without sample pretreatment.

1 Figure 3 displays normalized SERS spectra of fetuin and asialofetuin binding to 4MBA,
2 and the spectra of 1TBA, 3MBA, 4ABA, and PyriBA are shown in SI Figure 14. For 4MBA
3 spectra, sialic acid residues in fetuin cause the peak shifts to higher wavenumber and the
4 increases of intensity at 475 cm^{-1} (CCC out of plane bending) and 613 cm^{-1} (CCC in plane
5 bending). Similarly, the presence of sialic acid residues also results in the variations of
6 signal intensities at 1015 cm^{-1} (CC stretching, OH stretching) and at 1589 cm^{-1} (CC
7 stretching, CH bending). These spectral changes are consistent with the data of sialic acid
8 monosaccharide observed in our prior study¹⁵. For 1TBA, the spectra differences among
9 fetuin, asialofetuin, and negative control (no glycoprotein) are more significant. With sialic
10 acid residue, the lower spectral signals were observed at 431 cm^{-1} (CCCC torsion, SCCC
11 out-of-plane bending), 669 cm^{-1} (CCCC torsion, CCC in-plane bending), 1037 cm^{-1} (CC
12 stretching), 1125 cm^{-1} (CC stretching, HCC bending), and 1194 cm^{-1} (CC stretching). In
13 contrast, the signals raise at 1081 cm^{-1} (CC stretching) and 1554 cm^{-1} (CC stretching) when
14 sialic acid residues present. This changes are consistent with our prior observations of sialic
15 acid¹⁵.

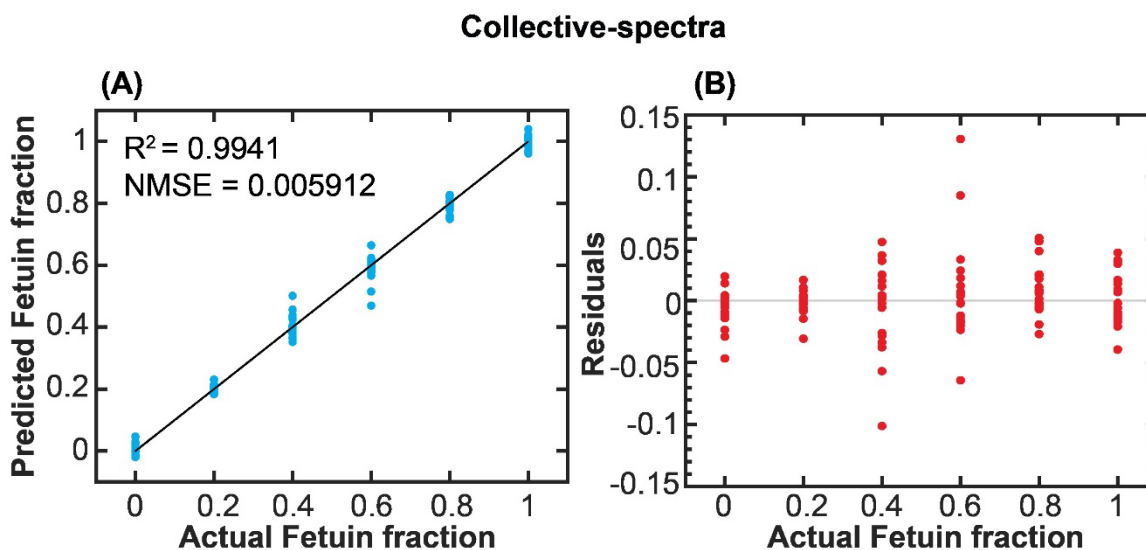
16 Since the presence of sialic acid residues in SERS spectra was observable, we evaluated
17 the capability of ML tool to quantify sialic acid levels in the samples containing both fetuin
18 and asialofetuin. Fetuin and asialofetuin were mixed with various molar ratios in total of 1
19 mM, and SERS spectra of the mixed samples were collected on the nanopapers
20 functionalized with different BAs. The sialic acid levels were quantified using Gaussian
21 regression models. SI Figure 15 illustrates the regression results using 4MBA, while SI
22 Figure 16 to SI Figure 19 show the results with 1TBA, 3MBA, 4ABA, and PyriBA. Among
23 the five BAs, 3MBA exhibit the best quantification performance, with R^2 of 0.9920 and
24 NMSE of 0.007982. This is probably because more spectral differences between fetuin and
25 asialofetuin were observed on 3MBA substrates, such as the peak intensity change around
26 785 cm^{-1} and 999 cm^{-1} . We also quantified the sialic acid levels using the collective spectra.
27 (Figure 4). As expected, the quantification result from the collective spectra of five BA
28 spectra is better than the analysis from the individual BA spectra.

29



1

2 Figure 3. Average normalized SERS spectra ($n=200$) of fetuin and asialofetuin on 4MBA coated substrates. Differences
 3 could be observed among 4MBA, 4MBA+fetuin, and 4MBA+asialofetuin spectra.



4

5 Figure 4 Predict fetuin fraction vs. actual fetuin fraction (A) and residual vs. actual fetuin fraction (B) for collective-
 6 spectra (4MBA, 1TBA, 3MBA, 4ABA, PyriBA) regression on fetuin fractions.

7

8 Sialic acid linkage identification

9 We have demonstrated this sensing platform can quantify sialylation levels of intact
 10 glycoproteins (mixtures of fetuin and asialofetuin). In our quest for deeper insights, we
 11 evaluate the capability of this sensing platform for distinguish sialic acid linkages. Sialic
 12 acids could link with other glycan entities in multiple linkage forms ($\alpha 2,3$, $\alpha 2,6$, $\alpha 2,8$ or
 13 $\alpha 2,9$)^{25, 27, 28}, and the most common linkages for sialic acids to other glycans are $\alpha 2,3$ and
 14 $\alpha 2,6$ ²⁵. It is crucial to differentiate sialic acids glycosidic linkages since the linkages could
 15 influence biological activities. For example, $\alpha 2,3$ linkage may promote selectin binding,
 16 and it is related to several cancers and higher patient death rates⁴⁶. Cancer cells are known
 17 to have high levels of $\alpha 2,6$ -linked sialic acid with galactose²⁵ and $\alpha 2,6$ linkage can block

1 the apoptosis inducing galectin proteins interactions with glycan, which improves cell
2 survival²⁷. The sialic acid linkage also impacts the anti-inflammatory properties of IgG.
3 IgG Fc fragments containing α 2,6-linked sialic acid only show a 10-fold increase in anti-
4 inflammatory activity compared to those containing both α 2,3- and α 2,6-linked sialic
5 acids⁴⁷. In contrast, Fc fragments containing only α 2,3-linked sialic acid show no anti-
6 inflammatory activity at all⁴⁷. It is crucial to ensure that the IgG antibodies used for anti-
7 inflammatory treatments have the appropriate sialic acid linkages through quality control.
8 IgG could be produced by HEK or CHO cell lines. However, CHO cell lines only produce
9 α 2,3-linked sialic acids while HEK cell lines could produce both types of linkage⁴⁸. As
10 such, identification of the sialic acid linkage is crucial for quality control in the
11 pharmaceutical industry. However, conventional LC-MS struggles to distinguish between
12 α 2,3 and α 2,6 linkages since they share the same molecular weight and result in identical
13 m/z values^{49, 50}. Having the ability to distinguish linkages with our platform will
14 significantly benefit the pharmaceutical industry and the glycobiology community.

15 The stereoselective reactions between BAs and glycans are determined by the spatial
16 orientations and intermolecular distance between BA moieties^{51, 52}. The recognition of α 2,3
17 and α 2,6 linkages could be improved by selecting appropriate BA receptors. To explore
18 this, we introduced three new BAs: PyreBA, HBACM, and BBA, alongside the five BAs
19 that are employed in the previous sections (4MBA, 1TBA, 3MBA, 4ABA, PyriBA)
20 (Structures are in SI Figure 1). PyreBA contains four aromatic rings, known for their
21 distinctive Raman vibrations⁵³. Using PyreBA as a model helps us understand the role of
22 aromatic ring vibrations in our platform. HBACM has been previously used in detecting
23 monosaccharides, such as glucose and fructose, as well as oligosaccharides like stachyose
24 and nystose^{54, 55}. Similarly, BBA closely resembles the structure of HBACM, with the
25 exception of a sulfur atom replacing the oxygen atom.

26 We examined the performance of the selected BAs in differentiating between the following
27 samples: 2,3 sialyllactose (3-SLA), 2,6 sialyllactose (6-SLA), and sialic acid
28 monosaccharide mixed with lactose (SA+Lac). (structure information are shown in SI
29 Figure 1). 3-SLA consists of a sialic acid residue attached to galactose in lactose molecule
30 with α 2,3 linkage, and 6-SLA has a α 2,6 linked sialic acid with lactose. To observe the
31 influence of sialic acid without linkage, we mixed the equal molar concentrations of sialic
32 acid monosaccharides with lactose.

33 SI Figure 20 and SI Figure 21 illustrate the confusion matrix and spectra for 4MBA and
34 1TBA. Both 1TBA and 4MBA successfully distinguished the existence of glycosidic
35 linkages. However, when it came to distinguishing the two different linkages, 4MBA
36 outperformed 1TBA. The difference may be attributed to the poor performance of 1TBA
37 in lactose identification shown in the previous study¹⁵. When we analyzed the collective
38 spectra, which incorporated the spectral data from both 4MBA and 1TBA, the accuracy
39 was improved. SI Figure 22 and SI Figure 23 showcase the confusion matrix and spectra
40 for 3MBA, 4ABA, and PyriBA, while SI Figure 24 and SI Figure 25 present the confusion
41 matrix and spectra for the new BAs, including PyreBA, HBACM, and BBA. Notably,

1 PyreBA did not exhibit strong classification performance. Conversely, both HBACM and
2 BBA delivered satisfactory results compared to the other tested BAs. Of particular interest,
3 3MBA, 4ABA, and BBA achieved a remarkable 100% accuracy. Finally, Figure 5 shows
4 the confusion matrix for the collective spectra of 8 boronic acids for sialic acid linkage
5 identification, which resulted in 100% accuracy as well. This discovery demonstrated that
6 the detection performance of the specific glycan structures can be improved by selecting
7 appropriate BA receptors, as well as the potential of using up to 8 boronic acids as an array
8 for glycan profiling.

9

Collective-spectra

True Class	SA+Lac	200		
	3SLA		200	
	6SLA			200
Sensitivity	100.0%	100.0%	100.0%	
Specificity	100.0%	100.0%	100.0%	
	SA+Lac	3SLA	6SLA	
	Predicted Class			

10

11 *Figure 5 Confusion matrix of sialic acid linkage classification using collective spectra method (100% accuracy) with all*
12 *8 boronic acids (4MBA, 1TBA, 3MBA, 4ABA, PyriBA, PyreBA, HBACM, and BBA).*

13

1 *Conclusion*

2 We have introduced a ML-driven SERS glycan sensor capable of classifying and
3 quantifying purified glycans with high accuracy¹⁵. Expanding upon this foundation, we
4 assessed the platform's ability to profile glycans in the presence of non-glycan entities.
5 Because SERS is a near-field phenomenon, the Raman signals are majorly contributed by
6 BA-glycan reaction complexes directly attached to the SERS substrates, and the influences
7 of background matrices are minimal. We successfully classified glycans in unprocessed
8 milk samples as well as quantified the sialylation level of intact glycoproteins (the mixture
9 of fetuin and asialofetuin). This discovery allows us to directly analyze biological samples
10 without time-consuming glycan releasing and extraction procedures. The elimination of
11 sample preparation steps would minimize the loss and degradation of glycans, eventually
12 reducing experimental variations.

13 BAs can reversibly bind with cis-diol in glycan molecules. By controlling spatial
14 orientations and intermolecular distance between BA moieties, BAs can bind to different
15 pairs of hydroxyl groups on a glycan with different binding affinities^{51, 52}. Different types
16 of BAs could yield different stereoselective reactions. In addition, most BAs contain
17 Raman active structures, so the BA-glycan reaction complexes could exhibit unique and
18 strong Raman spectral shifts. We hypothesize that detection accuracy can be improved by
19 integrating the Raman spectra collected from different BA receptors. To validate the
20 hypothesis, we established a sensor containing five different BAs to classify milk
21 oligosaccharides and quantify the sialylation levels of fetuin/asialofetuin mixtures. As
22 expected, the detection accuracy was significantly improved by integrating the spectral
23 data obtained from different BA receptors. This result offers a systematic strategy to
24 improve the sensor performance when the complexity of glycan sample increases.

25 We also explored how BA structures influence the detection of the glycosidic linkages. We
26 examined eight BA receptors containing various functional groups and aryl structures. The
27 appropriate BA receptors, including 3MBA, 4ABA, and BBA, could exhibit an excellent
28 performance of differentiating between α 2,3 and α 2,6 linkages of sialic acids. This
29 discovery suggested that the careful selection of BA receptors is crucial to improving the
30 detection accuracy.

31 In summary, the combination of SERS, BA receptors, and ML-driven chemometrics offers
32 a rapid and efficient approach for comparative glycan detection. This study demonstrated
33 this sensing platform could directly analyze unprocessed biological samples and intact
34 glycoproteins without glycan purification steps. We also demonstrate that the detection
35 accuracy can be improved by using multiple BA receptors. This sensor can serve as a rapid,
36 low-cost, and valuable tool for routine glycosylation analysis in standard laboratories.

37

1

Supporting Information

2 Peak assignments for 4MBA and 1TBA, Glycan and boronic acid structure, Scheme for
3 machine learning, SERS spectra for monosaccharides, electrostatic potential distribution
4 from DFT simulation, PCA contribution plots and confusion matrix for classification cases,
5 regression model performance plots (PDF)

6

7

Author Contributions

8 Q. Hu conducted the experiments and analyzed the data. Q. Hu and H.-J. Wu conceived
9 idea and wrote the manuscript.

10

11

Acknowledgements

12 The authors gratefully acknowledge the support from National Science Foundation (CBET-
13 2114203).

14

15

Notes

16 The authors declare no competing financial interest.

References

- (1) Gagneux, P.; Hennet, T.; Varki, A. Biological Functions of Glycans. *Essentials of Glycobiology [Internet]. 4th edition* **2022**.
- (2) Costa, A. R.; Rodrigues, M. E.; Henriques, M.; Oliveira, R.; Azeredo, J. Glycosylation: impact, control and improvement during therapeutic protein production. *Critical Reviews in Biotechnology* **2014**, *34* (4), 281-299. DOI: 10.3109/07388551.2013.793649.
- (3) Viinikangas, T.; Khosrowabadi, E.; Kellokumpu, S. N-Glycan Biosynthesis: Basic Principles and Factors Affecting Its Outcome. In *Antibody Glycosylation*, Pezer, M. Ed.; Springer International Publishing, 2021; pp 237-257.
- (4) Cummings, R. D.; Pierce, J. M. The challenge and promise of glycomics. *Chem Biol* **2014**, *21* (1), 1-15. DOI: 10.1016/j.chembiol.2013.12.010 From NLM Medline.
- (5) Marino, K.; Bones, J.; Kattla, J. J.; Rudd, P. M. A systematic approach to protein glycosylation analysis: a path through the maze. *Nat Chem Biol* **2010**, *6* (10), 713-723. DOI: 10.1038/nchembio.437 From NLM Medline.
- (6) Mimura, Y.; Katoh, T.; Saldova, R.; O'Flaherty, R.; Izumi, T.; Mimura-Kimura, Y.; Utsunomiya, T.; Mizukami, Y.; Yamamoto, K.; Matsumoto, T.; Rudd, P. M. Glycosylation engineering of therapeutic IgG antibodies: challenges for the safety, functionality and efficacy. *Protein Cell* **2018**, *9* (1), 47-62. DOI: 10.1007/s13238-017-0433-3 From NLM Medline.
- (7) Varki, A.; Cummings, R. D.; Esko, J. D.; Freeze, H. H.; Stanley, P.; Bertozzi, C. R.; Hart, G. W.; Etzler, M. E. Essentials of Glycobiology. In *Essentials of Glycobiology*, Varki, A., Cummings, R. D., Esko, J. D., Freeze, H. H., Stanley, P., Bertozzi, C. R., Hart, G. W., Etzler, M. E. Eds.; 2009.
- (8) Veillon, L.; Huang, Y.; Peng, W.; Dong, X.; Cho, B. G.; Mechref, Y. Characterization of isomeric glycan structures by LC-MS/MS. *ELECTROPHORESIS* **2017**, *38* (17), 2100-2114. DOI: <https://doi.org/10.1002/elps.201700042>.
- (9) Choi, H. K.; Lee, D.; Singla, A.; Kwon, J. S.; Wu, H. J. The influence of heteromultivalency on lectin-glycan binding behavior. *Glycobiology* **2019**, *29* (5), 397-408. DOI: 10.1093/glycob/cwz010 From NLM Medline.
- (10) Krishnan, P.; Singla, A.; Lee, C. A.; Weatherston, J. D.; Worstell, N. C.; Wu, H. J. Heteromultivalent binding of cholera toxin subunit B with glycolipid mixtures. *Colloids Surf B Biointerfaces* **2017**, *160*, 281-288. DOI: 10.1016/j.colsurfb.2017.09.035.
- (11) Worstell, N. C.; Krishnan, P.; Weatherston, J. D.; Wu, H. J. Binding Cooperativity Matters: A GM1-like Ganglioside-Cholera Toxin B Subunit Binding Study Using a Nanocube-Based Lipid Bilayer Array. *PLoS ONE* **2016**, *11* (4), e0153265. DOI: 10.1371/journal.pone.0153265.
- (12) Worstell, N. C.; Singla, A.; Saenkham, P.; Galbadage, T.; Sule, P.; Lee, D.; Mohr, A.; Kwon, J. S.; Cirillo, J. D.; Wu, H. J. Hetero-Multivalency of Pseudomonas aeruginosa Lectin LecA Binding to Model Membranes. *Scientific Reports* **2018**, *8* (1), 8419. DOI: 10.1038/s41598-018-26643-7.
- (13) Hirabayashi, J.; Yamada, M.; Kuno, A.; Tateno, H. Lectin microarrays: concept, principle and applications. *Chem Soc Rev* **2013**, *42* (10), 4443-4458, 10.1039/C3CS35419A. DOI: 10.1039/C3CS35419A.

- 1 (14) Dang, K.; Zhang, W.; Jiang, S.; Lin, X.; Qian, A. Application of Lectin Microarrays for
2 Biomarker Discovery. *ChemistryOpen* **2020**, *9* (3), 285-300. DOI:
3 <https://doi.org/10.1002/open.201900326>.
- 4 (15) Hu, Q.; Kuai, D.; Park, H.; Clark, H.; Balbuena, P. B.; Kwon, J. S.-I.; Wu, H.-J. Advancing
5 Glycan Analysis: A New Platform Integrating SERS, Boronic Acids, and Machine
6 Learning Algorithms. *Advanced Sensor Research* **2023**, *2* (12), 2300052. DOI:
7 <https://doi.org/10.1002/adsr.202300052>.
- 8 (16) Wang, X.; Xia, N.; Liu, L. Boronic Acid-based approach for separation and
9 immobilization of glycoproteins and its application in sensing. *Int J Mol Sci* **2013**, *14*
10 (10), 20890-20912. DOI: 10.3390/ijms141020890 PubMed.
- 11 (17) Melchiorre, M.; Ferreri, C.; Tinti, A.; Chatgililoglu, C.; Torreggiani, A. A Promising
12 Raman Spectroscopy Technique for the Investigation of trans and cis Cholesteryl Ester
13 Isomers in Biological Samples. *Appl Spectrosc* **2015**, *69* (5), 613-622. DOI: 10.1366/14-
14 07706 From NLM Medline.
- 15 (18) Cho, Y. C.; Ahn, S. I. Fabricating a Raman spectrometer using an optical pickup unit and
16 pulsed power. *Scientific Reports* **2020**, *10* (1), 11692. DOI: 10.1038/s41598-020-68650-
17 7.
- 18 (19) Weatherston, J. D.; Seguban, R. K. O.; Hunt, D.; Wu, H.-J. Low-Cost and Simple
19 Fabrication of Nanoplasmonic Paper for Coupled Chromatography Separation and
20 Surface Enhanced Raman Detection. *ACS Sensors* **2018**, *3* (4), 852-857. DOI:
21 10.1021/acssensors.8b00098 (accessed 2021-03-19T21:24:07).
- 22 (20) Weatherston, J. D.; Yuan, S.; Mashuga, C. V.; Wu, H.-J. Multi-functional SERS substrate:
23 Collection, separation, and identification of airborne chemical powders on a single device.
24 *Sensors and Actuators B: Chemical* **2019**, *297*, 126765. DOI:
25 <https://doi.org/10.1016/j.snb.2019.126765>.
- 26 (21) Saunders, M. J.; Woods, R. J.; Yang, L. Simplifying the detection and monitoring of
27 protein glycosylation during in vitro glycoengineering. *Scientific Reports* **2023**, *13* (1),
28 567. DOI: 10.1038/s41598-023-27634-z.
- 29 (22) Xu, M.; Yang, A.; Xia, J.; Jiang, J.; Liu, C.-F.; Ye, Z.; Ma, J.; Yang, S. Protein
30 glycosylation in urine as a biomarker of diseases. *Translational Research* **2023**, *253*, 95-
31 107. DOI: <https://doi.org/10.1016/j.trsl.2022.08.001>.
- 32 (23) Costa, J.; Hayes, C.; Lisacek, F. Protein glycosylation and glycoinformatics for novel
33 biomarker discovery in neurodegenerative diseases. *Ageing Research Reviews* **2023**, *89*,
34 101991. DOI: <https://doi.org/10.1016/j.arr.2023.101991>.
- 35 (24) Ghosh, S. Chapter 1 - Sialic acid and biology of life: An introduction. In *Sialic Acids and*
36 *Sialoglycoconjugates in the Biology of Life, Health and Disease*, Ghosh, S. Ed.;
37 Academic Press, 2020; pp 1-61.
- 38 (25) Lewis, A. L.; Chen, X.; Schnaar, R. L.; Varki, A. Sialic acids and other nonulosonic acids.
39 *Essentials of Glycobiology [Internet]*. 4th edition **2022**.
- 40 (26) Burzyńska, P.; Sobala, Ł. F.; Mikołajczyk, K.; Jodłowska, M.; Jaśkiewicz, E. Sialic acids
41 as receptors for pathogens. *Biomolecules* **2021**, *11* (6), 831.
- 42 (27) Wasik, B. R.; Barnard, K. N.; Parrish, C. R. Effects of Sialic Acid Modifications on Virus
43 Binding and Infection. *Trends in Microbiology* **2016**, *24* (12), 991-1001. DOI:
44 <https://doi.org/10.1016/j.tim.2016.07.005>.

- 1 (28) Schauer, R.; Kamerling, J. P. Chapter One - Exploration of the Sialic Acid World. In
2 *Advances in Carbohydrate Chemistry and Biochemistry*, Baker, D. C. Ed.; Vol. 75;
3 Academic Press, 2018; pp 1-213.
- 4 (29) Folch, J.; Lees, M.; Sloane Stanley, G. H. A simple method for the isolation and
5 purification of total lipides from animal tissues. *J Biol Chem* **1957**, 226 (1), 497-509. DOI:
6 [https://doi.org/10.1016/S0021-9258\(18\)64849-5](https://doi.org/10.1016/S0021-9258(18)64849-5) From NLM Medline.
- 7 (30) Nielsen, S. S. Phenol-Sulfuric Acid Method for Total Carbohydrates. In *Food Analysis*
8 *Laboratory Manual*, Food Science Texts Series, Springer US, 2010; pp 47-53.
- 9 (31) Jombart, T.; Devillard, S.; Balloux, F. Discriminant analysis of principal components: a
10 new method for the analysis of genetically structured populations. *BMC Genet* **2010**, 11
11 (1), 94. DOI: 10.1186/1471-2156-11-94 (accessed 2021-01-18T22:30:52). From NLM
12 Medline.
- 13 (32) Hu, Q.; Sellers, C.; Kwon, J. S.-I.; Wu, H.-J. Integration of surface-enhanced Raman
14 spectroscopy (SERS) and machine learning tools for coffee beverage classification.
15 *Digital Chemical Engineering* **2022**, 3, 100020. DOI:
16 <https://doi.org/10.1016/j.dche.2022.100020>.
- 17 (33) Berrar, D. Cross-Validation. In *Encyclopedia of Bioinformatics and Computational*
18 *Biology*, Ranganathan, S., Gribskov, M., Nakai, K., Schönbach, C. Eds.; Academic Press,
19 2019; pp 542-545.
- 20 (34) Guan, B.; Zhang, Z.; Chai, Y.; Amantai, X.; Chen, X.; Cao, X.; Yue, X. N-glycosylation
21 of milk proteins: A review spanning 2010–2022. *Trends in Food Science & Technology*
22 **2022**, 128, 1-21. DOI: <https://doi.org/10.1016/j.tifs.2022.07.017>.
- 23 (35) van Leeuwen, S. S.; te Poele, E. M.; Chatziioannou, A. C.; Benjamins, E.; Haandrikman,
24 A.; Dijkhuizen, L. Goat Milk Oligosaccharides: Their Diversity, Quantity, and Functional
25 Properties in Comparison to Human Milk Oligosaccharides. *Journal of Agricultural and*
26 *Food Chemistry* **2020**, 68 (47), 13469-13485. DOI: 10.1021/acs.jafc.0c03766.
- 27 (36) de Sousa, Y. R. F.; da Silva Vasconcelos, M. A.; Costa, R. G.; de Azevedo Filho, C. A.;
28 de Paiva, E. P.; Queiroga, R. d. C. R. d. E. Sialic acid content of goat milk during lactation.
29 *Livestock Science* **2015**, 177, 175-180. DOI: <https://doi.org/10.1016/j.livsci.2015.04.005>.
- 30 (37) Sheng, B.; Thesbjerg, M. N.; Glantz, M.; Paulsson, M.; Nielsen, S. r. D.; Poulsen, N. A.;
31 Larsen, L. B. Phosphorylation and glycosylation isoforms of bovine κ -casein variant E in
32 homozygous Swedish Red cow milk detected by liquid chromatography-electrospray
33 ionization mass spectrometry. *Journal of Dairy Science* **2022**, 105 (3), 1959-1965. DOI:
34 <https://doi.org/10.3168/jds.2021-21172>.
- 35 (38) Folch, J.; Lees, M.; Stanley, G. H. S. A SIMPLE METHOD FOR THE ISOLATION AND
36 PURIFICATION OF TOTAL LIPIDES FROM ANIMAL TISSUES. *Journal of*
37 *Biological Chemistry* **1957**, 226 (1), 497-509. DOI: [https://doi.org/10.1016/S0021-](https://doi.org/10.1016/S0021-9258(18)64849-5)
38 [9258\(18\)64849-5](https://doi.org/10.1016/S0021-9258(18)64849-5).
- 39 (39) Fischler, D. A.; Orlando, R. N-linked Glycan Release Efficiency: A Quantitative
40 Comparison between NaOCl and PNGase F Release Protocols. *J Biomol Tech* **2019**, 30
41 (4), 58-63. DOI: 10.7171/jbt.19-3004-001 From NLM.
- 42 (40) Kinoshita, M.; Yamada, K. Recent advances and trends in sample preparation and
43 chemical modification for glycan analysis. *Journal of Pharmaceutical and Biomedical*
44 *Analysis* **2022**, 207, 114424. DOI: <https://doi.org/10.1016/j.jpba.2021.114424>.

- 1 (41) Tiwold, E. K.; Gyorgypal, A.; Chundawat, S. P. S. Recent Advances in Biologic
2 Therapeutic N-Glycan Preparation Techniques and Analytical Methods for Facilitating
3 Biomanufacturing Automation. *J Pharm Sci-Us* **2023**, *112* (6), 1485-1491. DOI:
4 <https://doi.org/10.1016/j.xphs.2023.01.012>.
- 5 (42) Wilkinson, H.; Saldova, R. Current Methods for the Characterization of O-Glycans.
6 *Journal of Proteome Research* **2020**, *19* (10), 3890-3905. DOI:
7 10.1021/acs.jproteome.0c00435.
- 8 (43) Shipman, J. T.; Nguyen, H. T.; Desaire, H. So You Discovered a Potential Glycan-Based
9 Biomarker; Now What? We Developed a High-Throughput Method for Quantitative
10 Clinical Glycan Biomarker Validation. *ACS Omega* **2020**, *5* (12), 6270-6276. DOI:
11 10.1021/acsomega.9b03334.
- 12 (44) Lin, Y.-H.; Franc, V.; Heck, A. J. R. Similar Albeit Not the Same: In-Depth Analysis of
13 Proteoforms of Human Serum, Bovine Serum, and Recombinant Human Fetuin. *Journal*
14 *of Proteome Research* **2018**, *17* (8), 2861-2869. DOI: 10.1021/acs.jproteome.8b00318.
- 15 (45) Černocká, H.; Řimánková, L.; Ostatná, V. Fetuin and asialofetuin at charged surfaces:
16 Influence of sialic acid presence. *Journal of Electroanalytical Chemistry* **2021**, *902*,
17 115801. DOI: <https://doi.org/10.1016/j.jelechem.2021.115801>.
- 18 (46) Schultz, M. J.; Swindall, A. F.; Bellis, S. L. Regulation of the metastatic cell phenotype
19 by sialylated glycans. *Cancer and Metastasis Reviews* **2012**, *31* (3), 501-518. DOI:
20 10.1007/s10555-012-9359-7.
- 21 (47) Anthony, R. M.; Nimmerjahn, F.; Ashline, D. J.; Reinhold, V. N.; Paulson, J. C.; Ravetch,
22 J. V. Recapitulation of IVIG Anti-Inflammatory Activity with a Recombinant IgG Fc.
23 *Science* **2008**, *320* (5874), 373-376. DOI: doi:10.1126/science.1154315.
- 24 (48) Blundell, P. A.; Lu, D.; Dell, A.; Haslam, S.; Pleass, R. J. Choice of Host Cell Line Is
25 Essential for the Functional Glycosylation of the Fc Region of Human IgG1 Inhibitors of
26 Influenza B Viruses. *The Journal of Immunology* **2020**, *204* (4), 1022-1034. DOI:
27 10.4049/jimmunol.1901145 (accessed 1/29/2024).
- 28 (49) Manz, C.; Mancera-Arteu, M.; Zappe, A.; Hanozin, E.; Polewski, L.; Giménez, E.; Sanz-
29 Nebot, V.; Pagel, K. Determination of Sialic Acid Isomers from Released N-Glycans
30 Using Ion Mobility Spectrometry. *Analytical Chemistry* **2022**, *94* (39), 13323-13331.
31 DOI: 10.1021/acs.analchem.2c00783.
- 32 (50) Suzuki, N.; Abe, T.; Natsuka, S. Quantitative LC-MS and MS/MS analysis of sialylated
33 glycans modified by linkage-specific alkylamidation. *Analytical Biochemistry* **2019**, *567*,
34 117-127. DOI: <https://doi.org/10.1016/j.ab.2018.11.014>.
- 35 (51) Tommasone, S.; Allabush, F.; Tagger, Y. K.; Norman, J.; Köpf, M.; Tucker, J. H. R.;
36 Mendes, P. M. The challenges of glycan recognition with natural and artificial receptors.
37 *Chemical Society Reviews* **2019**, *48* (22), 5488-5505, 10.1039/C8CS00768C. DOI:
38 10.1039/C8CS00768C.
- 39 (52) Fang, G.; Wang, H.; Bian, Z.; Sun, J.; Liu, A.; Fang, H.; Liu, B.; Yao, Q.; Wu, Z. Recent
40 development of boronic acid-based fluorescent sensors. *RSC Advances* **2018**, *8* (51),
41 29400-29427, 10.1039/C8RA04503H. DOI: 10.1039/C8RA04503H.
- 42 (53) Nyquist, R. Chapter 9 - Benzene and Its Derivatives. In *Interpreting Infrared, Raman,*
43 *and Nuclear Magnetic Resonance Spectra*, Nyquist, R. A. Ed.; Academic Press, 2001; pp
44 351-423.

- 1 (54) Arimitsu, K.; Iwasaki, H.; Kimura, H.; Yasui, H. Strong Binding Affinity of d-Allulose
2 and Allulosides to Boronic Acids and the Structural Characterization of Their Sugar-
3 boronate Complexes. *Chemistry Letters* **2021**, *50* (8), 1470-1474. DOI:
4 10.1246/cl.210181 (accessed 1/11/2024).
- 5 (55) Tommasone, S.; Tagger, Y. K.; Mendes, P. M. Targeting Oligosaccharides and
6 Glycoconjugates Using Superselective Binding Scaffolds. *Adv Funct Mater* **2020**, *30* (31),
7 2002298. DOI: <https://doi.org/10.1002/adfm.202002298>.
- 8